

## SYMMETRIC AND NON-SYMMETRIC SATURATION\*

L. MOTYKA

DESY Theory Group, 22607 Hamburg, Germany  
andM. Smoluchowski Institute of Physics, Jagellonian University  
Reymonta 4, 30-059 Kraków, Poland  
motyka@th.if.uj.edu.pl*(Received October 16, 2006)*

An approach to the gluon saturation is discussed within a framework of interacting QCD pomeron field theory. The formulation is consistent with Lorentz invariance which guarantees that the symmetry between the target and the projectile of the scattering matrix is preserved. The dynamics of interacting pomeron system is studied in the semi-classical approximation. Solutions to the emerging classical equations of motion (Braun equations) are presented. Two unexpected features of these solutions are found: a break-down of the symmetry between the target and the projectile and their similarity to solutions of the Balitsky–Kovchegov equation. Interpretation of the results is given and possible consequences are shortly discussed.

PACS numbers: 24.80.+y, 24.85.+p, 11.80.La

**1. Introduction**

Description of chromodynamic interactions in high energy hadron and nucleus scattering may be conveniently organised in a framework of effective field theory of interacting QCD pomerons [1–3]. The basic degree of freedom — the QCD pomeron — is a compound colour singlet state that consists of two reggeized gluons interacting with each other by an exchange of elementary gluons. The QCD evolution of this ladder-like system, that resums leading logarithms of the scattering energy squared,  $s$ , is described by the BFKL equation [4]. The BFKL pomeron alone, however, is not sufficient to maintain the unitarity of the  $S$ -matrix. It is clearly visible from a power-like growth of the single BFKL pomeron exchange with energy — at

---

\* Presented at the XLVI Cracow School of Theoretical Physics, Zakopane, Poland May 27–June 5, 2006.

a fixed impact parameter the BFKL amplitude behaves like  $s^\lambda$  with  $\lambda \sim 0.3$ , and this behaviour would eventually lead to unitarity breaking.

The unitarity of effective pomeron field theory (PFT) is preserved if interactions of pomerons are suitably incorporated. The lowest order vertices are triple pomeron vertices corresponding to the pomeron merging and splitting [5]. Arbitrariness of the choice of the target and the projectile, and thus of the direction of the evolution variable in the rapidity evolution, implies that the vertices for pomeron merging and splitting are uniquely related to each other. In more general terms, the action of PFT exhibits the target-projectile symmetry [6].

The complete evaluation of scattering amplitudes in PFT is rather difficult as it amounts to solving non-local quantum field theory. In the diagrammatic language it means that all the pomeron Feynman diagrams with arbitrary topology should be resummed, and the generic diagrams contain closed pomeron loops (see Fig. 1(c)). An essential simplification of the theory is obtained if the vertex for the pomeron splitting is neglected. Then, the pomeron loops cannot be formed and only fan diagrams, shown in Fig. 1(a), contribute to scattering amplitudes. This is a suitable approximation for a description of high energy scattering of a small colour probe (*e.g.* a small colour dipole) off an extended large target (*e.g.* a nucleus), and a resummation of such diagrams leads to the Balitsky–Kovchegov (BK) equation [7, 8]. Let us stress that the BK limit requires that independent couplings of many pomerons to the target are possible. Note, that the BK problem is, in terms of PFT, a classical problem — only the pomeron diagrams with the tree topology contribute.

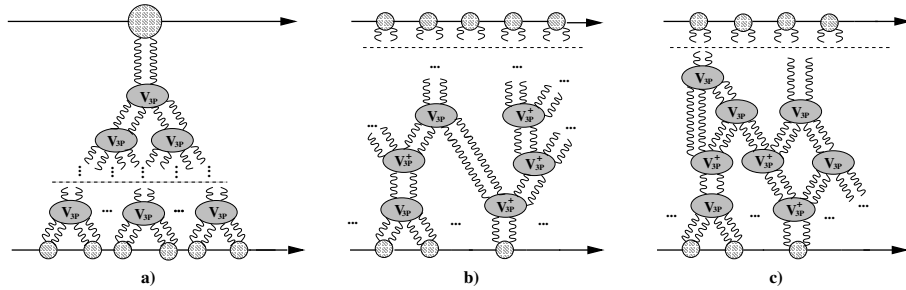


Fig. 1. Examples of diagrams of the effective field theory of QCD pomerons interacting with triple pomeron vertices: (a) a fan diagram; (b) a tree diagram defining the classical limit; (c) a diagram with quantum loops.

A natural next step in the analysis of PFT, beyond the BK equation, is to consider pomeron tree diagrams (see Fig. 1(b)) in the complete theory whose dynamics embodies both merging and splitting of the pomerons.

A resummation of such diagrams is equivalent to solving classical equations of motion in PFT (Braun equations), firstly derived by Mikhail Braun [2]. It was also argued [2] that the semi-classical approximation should provide a reasonable description of the scattering amplitude in nucleus–nucleus collisions. Possible phenomenological applications of the formalism remain to be studied, however, and in this contribution, we shall focus on a construction of pomeron field theory with the pomeron merging and splitting on the analysis of solutions of the Braun equations. The results presented below are based on our recently completed work [3].

It is important to stress here that the field-theoretical approach to QCD saturation is not the only one. In fact, much more activity has been devoted to studies of the  $s$ -channel picture of high energy scattering [9] which developed into the Colour Glass Condensate (CGC) formulation [10,11]. This very successful framework explores the connection of high energy scattering to dynamics of stochastic systems [11]. A description of the framework and recent developments may be found for instance in lectures given during the School [12–14]. The relation of the CGC to PFT is an important issue. In principle, both formulations are based on the same underlying gauge theory and use similar approximations — so one expects that the formulations are equivalent. Some evidence that supports that, indeed, the equivalence occurs follows from the fact that both the approaches lead, in the suitable limit, to the BK equation. Thus, the triple pomeron vertices responsible for the pomeron merging are equivalent in the PFT and in the CGC [15]. Furthermore, in both the approaches the vertex for pomeron splitting is uniquely determined by the symmetry between the target and the projectile and the vertex for pomeron merging. Therefore, although no explicit proof exists, one expects that up to triple pomeron vertices the CGC and PFT formulations agree.

So far, we discussed mostly the dynamics of the rapidity evolution of the interacting pomeron system. The complete formulation of the scattering problem requires, however, that the (multiple) couplings of the pomerons to external sources are specified. Naively, one would start from eikonal couplings, meaning that the multi-pomeron coupling factorises (up to the combinatoric symmetry factor) into the product of the independent single pomeron couplings. Consequently, an arbitrary large number of the pomerons could couple to the source at given impact parameter. This assumption, however, is invalid in the case of the source given by an elementary colour dipole. An elementary colour dipole may be coupled (at the leading logarithmic approximation) only to a single BFKL pomeron [1, 16]. This is a consequence of the bootstrap equation describing the gluon reggeisation. Clearly, this implies that the unitarisation of the dipole-dipole scattering in QCD cannot be achieved without pomeron loops and therefore the semi-classical

approach is useless in this case. The situation is different for an extended and complex object, like a nucleus. Then, the eikonal multi-pomeron coupling may provide a reasonable approximation. In fact, this assumption was used by Kovchegov in his derivation of the BK equation [8]. Thus, a non-trivial application of Braun equations is possible only to a scattering of two large and complex objects, like two nuclei. This situation is very different from problems typically considered in the CGC formulation: a small dipole-nucleus (or a small dipole-nucleon) scattering or dipole-dipole scattering, and this should be kept in mind when the results obtained within those two approaches are compared.

The paper is organised as follows. In the next section the formalism of effective QCD pomeron field theory is presented and the Braun equations are derived. In Sec. 3 solutions of the Braun equations are described. In Sec. 4 we provide some insight into the results of Sec. 3 coming from a toy model of reggeon field theory in zero transverse dimensions. Concluding remarks are given in Sec. 5.

## 2. Effective action of pomeron field theory

A convenient starting point for a construction of the effective action of PFT is the BK equation. In the initial formulation the BK equation described the rapidity evolution of the dipole scattering amplitude off a large target,  $N(y; \mathbf{r}, \mathbf{b})$ , where the dipole spans the vector  $\mathbf{r}$  and it is located at the transverse position  $\mathbf{b}$ . We will, however, use the representation [17] of the BK equation in which the basic degree of freedom is an unintegrated gluon density  $f(y, k^2, \mathbf{b})$  depending on the rapidity  $y$ , the gluon virtuality  $k^2$  and the transverse position  $\mathbf{b}$ . The unintegrated gluon density in the transverse space may be related in the small- $x$  limit to the collinear gluon distribution of the target  $A$

$$\int_A d^2\mathbf{b} f(y, k^2, \mathbf{b}) = \frac{\partial x g(x, k^2)}{\partial \log k^2}, \quad (1)$$

where  $y = \log(1/x)$ . For the large target one may assume that the target is locally uniform and that the evolution of  $N(y; \mathbf{r}, \mathbf{b})$  is approximately local in  $\mathbf{b}$ , so  $\mathbf{b}$  enters only through the initial condition. Thus, in the following analysis the argument  $\mathbf{b}$  of the gluon density will be suppressed. In this representation the BK equation reads ( $a^2$ ,  $b^2$  and  $c^2$  below denote gluon virtualities) [17]

$$\begin{aligned} \partial_y f(y, k^2) = & \int \frac{da^2}{a^4} \mathcal{K}_0(k^2, a^2) f(y, a^2) - 2\pi\alpha_s^2 \left[ k^2 \int_{k^2} \frac{da^2}{a^4} f(y, a^2) \right. \\ & \left. \times \int_{k^2} \frac{db^2}{b^4} f(y, b^2) + f(y, k^2) \int_{k^2} \frac{da^2}{a^4} \log\left(\frac{a^2}{k^2}\right) f(y, a^2) \right], \end{aligned} \quad (2)$$

and  $\mathcal{K}_0$  is the amputated forward BFKL kernel given by

$$\int \frac{db^2}{b^4} \mathcal{K}_0(a^2, b^2) f(b^2) = \frac{N_c \alpha_s}{\pi} a^2 \int \frac{db^2}{b^2} \left[ \frac{f(b^2) - f(a^2)}{|b^2 - a^2|} + \frac{f(a^2)}{[4b^4 + a^4]^{\frac{1}{2}}} \right]. \quad (3)$$

It is easy to verify that the nonlinear term describing joining of two pomerons,  $(f, f) \rightarrow f$  is generated from the amplitude of the Bartels triple pomeron vertex [5] (in the forward limit),

$$\begin{aligned} (f^\dagger | V_{3P} | f \otimes f) = & -2\pi\alpha_s^2 \int \frac{da^2}{a^4} a^2 f^\dagger(y, a^2) \int_{a^2} \frac{db^2}{b^4} f(y, b^2) \int_{a^2} \frac{dc^2}{c^4} f(y, c^2) \\ & - 2\pi\alpha_s^2 \int \frac{da^2}{a^4} f^\dagger(y, a^2) f(y, a^2) \int_{a^2} \frac{db^2}{b^4} \log\left(\frac{b^2}{a^2}\right) f(y, b^2) \end{aligned} \quad (4)$$

by functional differentiation with respect to the auxiliary pomeron field  $f^\dagger(y, k^2)$ . In fact, beyond the BK limit, it is necessary to consider the dynamics of the field  $f^\dagger(y, k^2)$  and it turns out the fields  $f(y, k^2)$  and  $f^\dagger(y, k^2)$  may be interpreted as the Gribov fields.

The BK equation accounts only for the pomeron merging. Construction of triple pomeron vertex for the pomeron splitting is easy. Namely, in order to distinguish merging of the pomerons from a splitting of a pomeron the direction of the evolution in rapidity must be specified. This choice is, however, completely arbitrary and the form the action should not depend on it. In consequence, the effective action is invariant under the transform,

$$f \leftrightarrow f^\dagger, \quad y \rightarrow -y, \quad (5)$$

and the form of the splitting vertex  $(f^\dagger \otimes f^\dagger | V_{3P}^\dagger | f)$  is given by  $(f^\dagger | V_{3P} | f \otimes f)^\dagger$ .

Thus, neglecting all multi-pomeron vertices higher than the triple pomeron vertices one obtains the effective action of PFT in the following form:

$$\mathcal{A}[f, f^\dagger; Y] = \frac{4\pi^3}{N_c^2 - 1} \int_0^Y dy \left\{ \mathcal{L}_0[f, f^\dagger] + \mathcal{L}_3[f, f^\dagger] + \mathcal{L}_3^\dagger[f, f^\dagger] + \mathcal{L}_E[f, f^\dagger] \right\}, \quad (6)$$

where the Lagrange function for the free propagation reads

$$\begin{aligned} \mathcal{L}_0[f, f^\dagger] &= \frac{1}{2} \int \frac{da^2}{a^4} \left[ f(y, a^2) \partial_y f^\dagger(y, a^2) - f^\dagger(y, a^2) \partial_y f(y, a^2) \right] \\ &+ \int \frac{da^2}{a^4} \int \frac{db^2}{b^4} f^\dagger(y, a^2) \mathcal{K}_0(a^2, b^2) f(y, b^2). \end{aligned} \quad (7)$$

The Lagrange function describing merging of two pomerons takes the form

$$\mathcal{L}_3[f, f^\dagger] = (f^\dagger | V_{3P} | f \otimes f), \quad (8)$$

and splitting of a pomeron contributes with

$$\mathcal{L}_3[f, f^\dagger] = (f^\dagger \otimes f^\dagger | V_{3P} | f). \quad (9)$$

The coupling of the pomerons to the external sources is represented by

$$\mathcal{L}_E[f, f^\dagger] = \int \frac{da^2}{a^4} \left[ f_E^\dagger(y, a^2) f(y, a^2) + f^\dagger(y, a^2) f_E(y, a^2) \right], \quad (10)$$

where the external sources will be assumed to be localised in rapidity,

$$f_E(y, a^2) = f_A(a^2) \delta(y), \quad f_E^\dagger(y, a^2) = f_B^\dagger(a^2) \delta(y - Y). \quad (11)$$

Clearly,  $f_A$  represents the amplitude of emission of the pomeron described by the field  $f(y, k^2)$  from the source at  $y = 0$  and  $f_B^\dagger$  is the coupling of  $f^\dagger(y, k^2)$  to an external source at  $y = Y$ .

The elements of the action are graphically represented in Fig. 2.

The action lacks the appropriate treatment of the transverse position and thus it is not suitable to describe the pomeron quantum loops, for which correlations of the pomerons in the transverse plane are essential. Nevertheless, the action treated in the semi-classical framework may be used to approximately resum the BFKL pomeron tree diagrams (see Fig. 1(b)) in scattering of two large objects, for instance of two nuclei. For a scattering in which the projectile and the target have sizes much larger than the typical momenta in the QCD pomeron, the momentum transfer any pomeron line

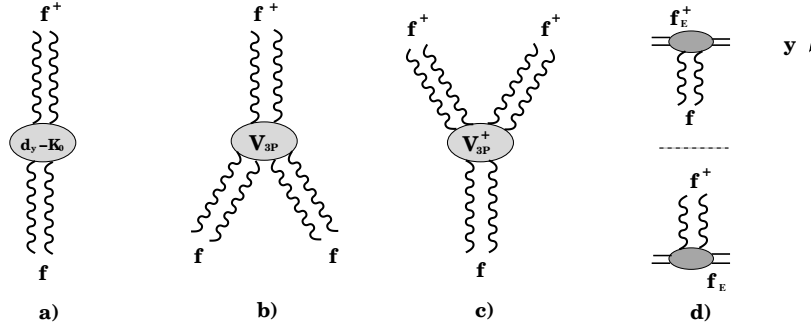


Fig. 2. Elements of the effective action: (a) the BFKL pomeron propagator; (b) the merging vertex; (c) the splitting vertex and (d) the external sources of the fields. The arrow indicates the direction of evolution.

originating from the external particles is bounded to be small by the form-factors of the sources and it may be therefore neglected.

Let us return to the symmetry of the action defined by Eq. (5). This symmetry causes the action to be self-dual [6]. Indeed, after integration by parts of the “time derivative” part of the action

$$\int_0^Y dy \frac{1}{2} \left[ f(y, a^2) \partial_y f^\dagger(y, a^2) - f^\dagger(y, a^2) \partial_y f(y, a^2) \right] \tag{12}$$

is transformed to

$$\int_0^Y dy \left[ -f^\dagger(y, a^2) \partial_y f(y, a^2) \right] + (\dots), \tag{13}$$

where (...) denote the boundary terms, and one gets that

$$\frac{\delta \mathcal{L}[f, f^\dagger]}{\delta(\partial_y f(y, k^2))} = -\frac{1}{k^4} f^\dagger(y, k^2). \tag{14}$$

This means, that the field  $f^\dagger(y, k^2)$  is the canonical conjugate of  $f(y, k^2)$ , up to the factor of  $1/k^4$  which can be easily absorbed into the field definitions and trivial complex phase factors. After invoking the symmetry (5) we conclude that the bulk part of the action (6) may be rewritten in the self-dual form. The symmetry of the action (6) may be completed by assuming the

symmetric external sources, that enter  $\mathcal{L}_E$ . Then, one expects the solution of the field equations  $\{f, f^\dagger\}$  to be also symmetric

$$f(y, k^2) = f^\dagger(Y - y, k^2), \quad (15)$$

that is one expects that the target-projectile symmetry is realized at the level of the solutions of the Braun equations.

The equations of motion read [3]:

$$\partial_y f(y, k^2) = [\mathcal{K}_0 \otimes f](y, k^2) + \frac{\delta(f^\dagger | V_{3P} | f \otimes f)}{\delta f^\dagger(y, k^2)} + \frac{\delta(f^\dagger \otimes f^\dagger | V_{3P} | f)}{\delta f^\dagger(y, k^2)}, \quad (16)$$

$$-\partial_y f^\dagger(y, k^2) = [\mathcal{K}_0 \otimes f^\dagger](y, k^2) + \frac{\delta(f^\dagger | V_{3P} | f \otimes f)}{\delta f(y, k^2)} + \frac{\delta(f^\dagger \otimes f^\dagger | V_{3P} | f)}{\delta f(y, k^2)} \quad (17)$$

with two-point boundary conditions,

$$f(y = 0, k^2) = f_A(k^2), \quad f^\dagger(y = Y, k^2) = f_B^\dagger(k^2). \quad (18)$$

The equations are equivalent to the equations derived by Braun [2], although they are formulated here using other variables. Therefore we shall refer to equations (16), (17) as to the Braun equations. The interpretation of the degrees of freedom that we use is straightforward in terms of perturbative QCD in the momentum space; the basic physical objects: the unintegrated gluon density and the triple pomeron vertex in the momentum space are represented in a transparent way.

Solutions to the classical equations of motion for the pomeron fields may be used to determine the  $S$ -matrix for the high energy scattering in the semi-classical approximation. In order to do that, however, the dependence of the problem on the transverse position has to be taken into account.

Thus, assuming locality of the evolution in the transverse space the complete action takes the form

$$\tilde{\mathcal{A}}[f, f^\dagger; Y, \mathbf{b}] = \int d^2 \mathbf{b}_1 \mathcal{A}[f(y, k^2, \mathbf{b}_1), f^\dagger(y, k^2, \mathbf{b} - \mathbf{b}_1); Y], \quad (19)$$

where the equations of motion may be employed to obtain

$$\mathcal{A}[f, f^\dagger; Y] = \frac{1}{2} \int_{0^-}^{Y^+} dy \left\{ \mathcal{L}_E[f, f^\dagger] - \mathcal{L}_3[f, f^\dagger] - \mathcal{L}_3^\dagger[f, f^\dagger] \right\}, \quad (20)$$

leading, in the semi-classical approximation, to the  $S$ -matrix

$$S(Y, \mathbf{b}) = \exp\{-\tilde{\mathcal{A}}[f, f^\dagger; Y, \mathbf{b}]\}. \quad (21)$$

### 3. Solutions of the Braun equations

Classical equations of motion (16) and (17) for the effective pomeron fields  $f(y, k^2)$  and  $f^\dagger(y, k^2)$  were solved numerically for various values of the total rapidity  $Y$  between the target and the projectile [3]. All the results were obtained assuming the fixed coupling constant  $\alpha_s = 0.2$ . As the default case, we applied the initial conditions (18) in the form:

$$f_A(k^2) = f_B^\dagger(k^2) = N_0 \frac{k^4}{Q_0^4 + k^4}. \quad (22)$$

This condition was inspired by the properties of a saturated gluon distribution in the nucleon. Thus we set  $Q_0^2 = 0.5 \text{ GeV}^2$ , which corresponds to the saturation scale in the nucleon gluon density at  $10^{-3} < x < 10^{-2}$ , and  $N_0 \simeq 0.08 \text{ GeV}^2$ , so that the collinear gluon distribution obtained from the input is similar to the actual collinear gluon distribution  $xg(x, Q^2)$  in the proton for  $10^{-3} < x < 10^{-2}$  and for moderate  $Q^2$ . The small- $k^2$  asymptotics,  $\sim k^4$ , was chosen for consistence with the behaviour of the gluon density that emerges from the BK equation, and at the large  $k^2$  a flat behaviour of  $f_A(k^2)$  was assumed, a natural choice which follows from an absence of the QCD evolution in the initial gluon distribution. The numerical solution was based on a Chebyshev interpolation method in the variable  $\log(k^2)$  used to discretise the differentio-integral equations (16) and (17). In order to effectively deal with the initial conditions imposed at two points of rapidity an iterative procedure was applied which turned out to be convergent and stable. The details of the solving procedure and the complete discussion of the solutions is given in Ref. [3]. Various boundary conditions, besides (22) were investigated and the qualitative features of the solutions did not depend on the details. Here we shall focus on the most striking properties of the solutions: a spontaneous breaking of the symmetry between the target and the projectile at the level of classical solutions and a fan dominance property.

The action of PFT, and consequently, the Braun equations are symmetric under the target-projectile symmetry. Therefore, naively, one expects that if a symmetric initial conditions are assumed,  $f_A(k^2) = f_B(k^2)$ , then the solution of the Braun equations is also symmetric,  $f^\dagger(y, k^2) = f(Y - y, k^2)$ . Indeed, this is true if the total rapidity  $Y$  is small enough. Above certain critical rapidity  $Y_c$ , however, this simple pictures breaks down and the solutions of Braun equations are asymmetric,  $f^\dagger(y, k^2) \neq f(Y - y, k^2)$ .

In Fig. 3 the solutions to the Braun equations for  $Y = 8$  are shown. Solid lines denote  $f(y, k^2)/k^2$ , and  $f^\dagger(y', k^2)/k^2$  — with  $y' = Y - y$  — is shown with points. The curves are plotted for  $y$  varying from zero to  $Y$  in the steps of one. The curve labelled the ‘‘Input’’ shows  $f_A(k^2)/k^2$ , where  $f_A(k^2)$  is

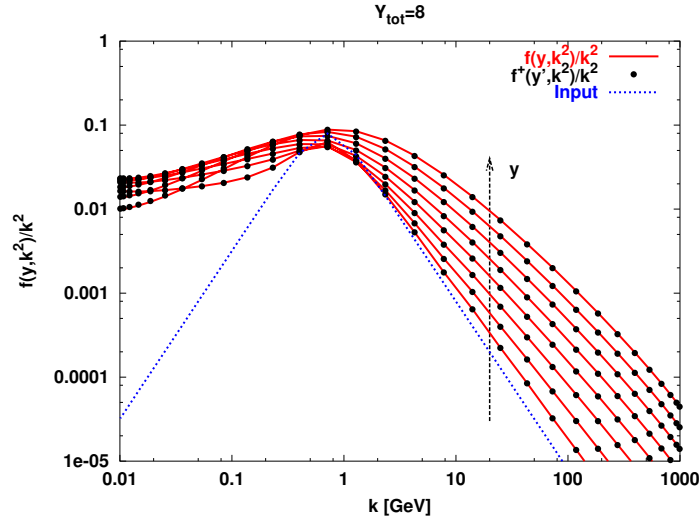


Fig. 3. Solutions of the Braun equations  $f(y, k^2)/k^2 = f^\dagger(y', k^2)/k^2$  for  $Y = 8$ .

defined by (22). Clearly, the solution is symmetric,  $f(y, k^2) = f^\dagger(Y - y, k^2)$ . Both components of the solutions exhibit a similar behaviour to a solution of the BK equation at large gluon momenta  $k^2$ . At small momenta, below the saturation scale of the BK equation,  $f(y, k^2)$  and  $f^\dagger(y', k^2)$  are much flatter than  $f^{\text{BK}}(y, k^2)$ , the solution to the BK equation with the input given by (22). It turns out that the symmetry between  $f$  and  $f^\dagger$  breaks down at certain critical rapidity  $Y_c \simeq 9$ , for our choice of the initial conditions. For  $Y > Y_c$  only asymmetric solutions were found with our method, for which  $f(y, k^2) \neq f^\dagger(Y - y, k^2)$ , compare Fig. 4(a) and Fig. 4(b), which illustrate  $f(y, k^2)/k^2$  and  $f^\dagger(y, k^2)/k^2$  respectively, for  $Y = 16$ . Note that, the initial condition for  $f$  appears at  $y = 0$  in Fig. 4(a) and the input of  $f^\dagger$  is plotted for  $y = 16$  in Fig. 4(b).

From Fig. 4 one sees that the symmetry between the target and the projectile is spontaneously broken for individual classical solutions. In more detail, the components of the asymmetric solution  $f(y, k^2)$  and  $f^\dagger(Y - y, k^2)$  approach each other for  $Y \rightarrow Y_c^+$ , and the asymmetric solution connects smoothly to the symmetric solution at  $Y \rightarrow Y_c^-$ . The asymmetry builds up gradually with increasing  $Y$  and is very large for  $Y \gg Y_c$ . Certainly, the numeric value of the critical rapidity  $Y_c$  is not universal, it depends on the initial conditions and on the value of  $\alpha_s$ . It is important to note, that for each asymmetric solution  $\{f, f^\dagger\}$  there exists a complementary solution  $\{f', f'^\dagger\}$ , such that  $f'(y, k^2) = f^\dagger(Y - y, k^2)$  and  $f'^\dagger(Y - y, k^2) = f(y, k^2)$ , reflecting the symmetry between the projectile and the target encoded in the

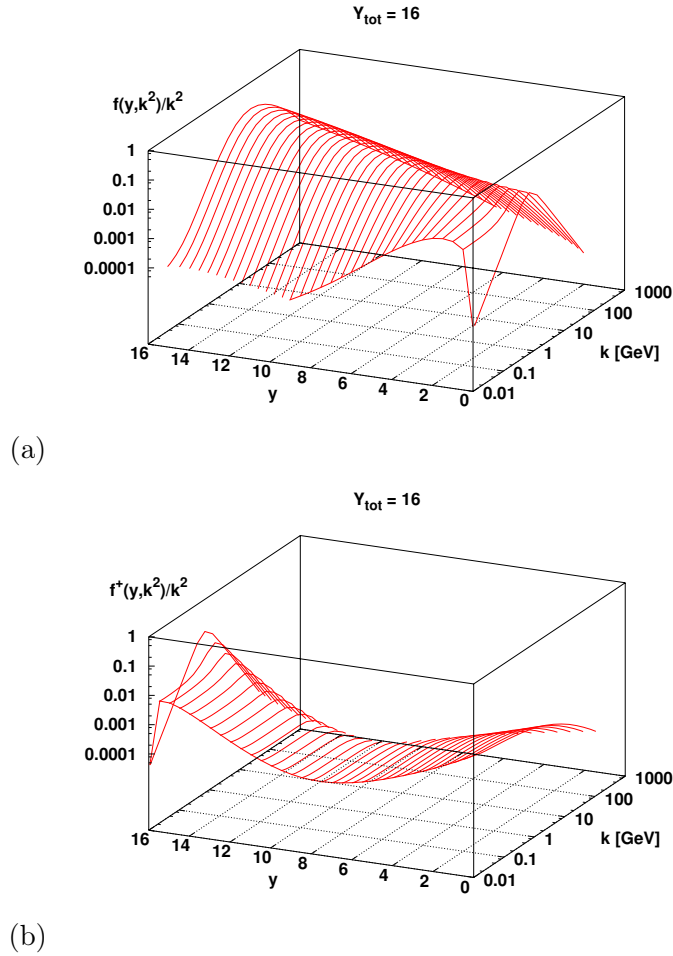


Fig. 4. Solutions of the Braun equations for  $Y = 16$  plotted as a function of rapidity  $y$  and  $k$ : a)  $f(y, k^2)/k^2$  and b)  $f^\dagger(y, k^2)/k^2$ .

action and the symmetric initial conditions. Knowing that, in the further analysis of the solutions we choose arbitrarily that  $f(y, k^2)$  is the larger field and  $f^\dagger(y', k^2)$  is the smaller one.

For  $Y > Y_c$ , the general features of the larger field  $f$  are the following. At  $Y \simeq Y_c$  the solution is similar to the symmetric solutions found for  $Y < Y_c$ . With increasing  $Y$  a pattern appears of a travelling wave, that is formation of a peak of  $f(y, k^2)/k^2$  travelling towards larger values of  $\log(k^2)$  with increasing rapidity with only small changes of the shape, see Fig. 5(a). Recall, that it is behaviour characteristic for solutions of the BK equation [18].

The smaller field  $f^\dagger(y, k^2)$  evolves in a different manner. For  $Y > Y_c$  it experiences a significant overall suppression, that increases with increasing  $Y$ . For instance, at  $Y = 16$  and for  $y \simeq 8$  the maximal value of  $f^\dagger(y, k^2)/k^2$  is about three orders of magnitude smaller than the maximal value of  $f(y, k^2)/k^2$ . The shape of  $f^\dagger(y', k^2)/k^2$  in  $k^2$  exhibits some inter-

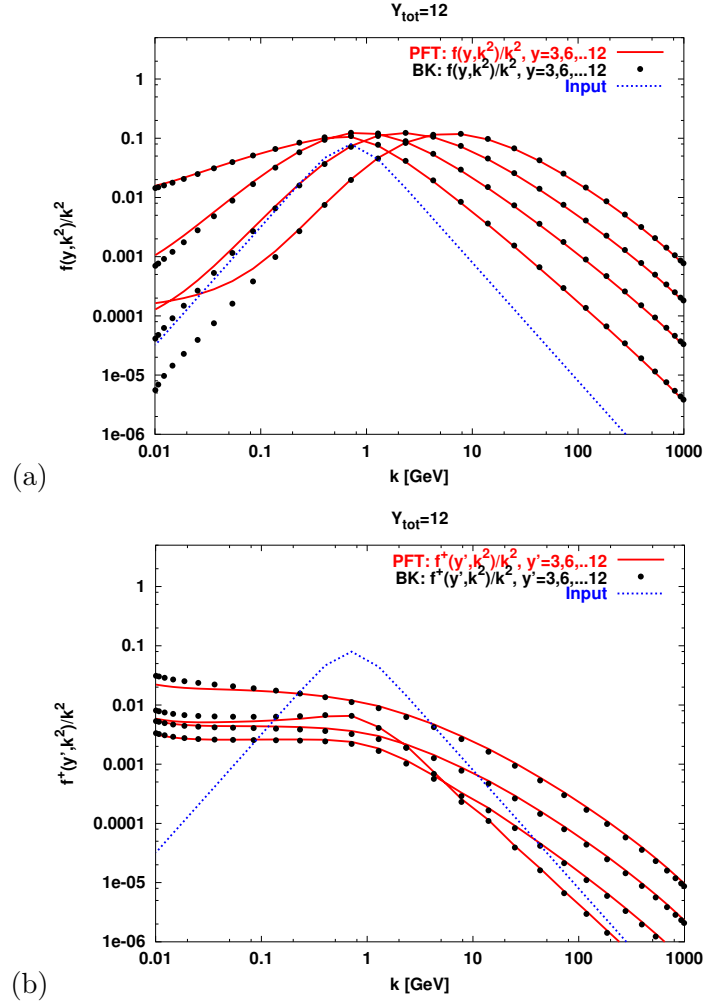


Fig. 5. Comparison of solutions of the Braun equations (solid line) to the solution of the BK equation (points) for  $Y = 12$ : (a) the larger solution  $f(y, k^2)/k^2$  and (b) the smaller solution  $f^\dagger(y, k^2)/k^2$ .

esting features. At small values of  $k^2$ ,  $f^\dagger(y', k^2)/k^2$  tends to a flat function. This should be compared with the case of the BK where  $f^{\text{BK}}(y, k^2)/k^2 \sim k^2$  at small  $k^2$ . On the other hand, at large  $k^2$  the decrease of  $f^\dagger(y', k^2)/k^2$  with increasing  $k^2$  is slower than the decrease of  $f^{\text{BK}}(y, k^2)/k^2$ . Thus, the overall picture is that  $f^\dagger(y', k^2)/k^2$  is much flatter than  $f^{\text{BK}}(y, k^2)/k^2$ .

We have already related briefly the larger component  $f(y, k^2)$  of the solution to the Braun equations to the solution of the Balitsky–Kovchegov equation  $f^{\text{BK}}(y, k^2)$ . A more detailed comparison is performed in Fig. 5 for  $Y = 12$ . Clearly, both  $f(y, k^2)$  and  $f^\dagger(y', k^2)$  are very similar to the corresponding components of the BK solution,  $f^{\text{BK}}(y, k^2)$  and  $f^{\dagger\text{BK}}(y', k^2)$ <sup>1</sup>. Some small deviations are visible only for very small gluon momenta and  $y > Y/2$ . In fact, both the overlap between  $f(y, k^2)$  and  $f^{\text{BK}}(y, k^2)$  and between  $f^\dagger(y', k^2)$  and  $f^{\dagger\text{BK}}(y', k^2)$  further improves with growing  $Y$ , and at  $Y \gg Y_c$  one expects that the differences between solutions of the Braun equations and solutions of the BK equation are negligible. This property will be referred to as a “fan dominance”.

#### 4. Reggeon field theory in zero transverse dimensions

The results that we have found in the case of PFT are somewhat surprising at the first sight, in particular the lack of the target-projectile symmetry in the classical field trajectories calls for an explanation. Therefore it should be useful to study a simpler analogue of PFT — reggeon field theory in zero transverse dimensions (RFT-0). This model was formulated and thoroughly analysed long time ago [19, 20] but it attracts some attention also nowadays [21]. The dynamics of RFT-0 is driven by the action

$$\mathcal{A}_{\text{RFT-0}}[q(y), p(y); Y] = \int_0^Y dy \mathcal{L}_{\text{RFT-0}}, \quad (23)$$

with the Lagrangian:

$$\mathcal{L}_{\text{RFT-0}} = \frac{1}{2} q \partial_y p - \frac{1}{2} p \partial_y q + \mu q p - \lambda q (q + p) p + q_0 p + q p_0, \quad (24)$$

where  $\mu$  is the intercept of the pomeron,  $\lambda$  is the triple pomeron coupling and  $\{q, p\}$  are (up to complex phase factors) Gribov fields depending only on rapidity and responsible for the creation and annihilation of pomerons. They correspond to  $f$  and  $f^\dagger$  of pomeron field theory. The functions  $q_0(y)$

---

<sup>1</sup> Evolution of the smaller component  $f^{\dagger\text{BK}}(y', k^2)$  in the BK limit was performed by solving the system (16) and (17) with the terms neglected that were generated by the triple pomeron vertex corresponding to the pomeron splitting (the contribution to the action of  $\mathcal{L}_3^\dagger$ ).

and  $p_0(y)$  are the external sources of the  $q$  and  $p$  fields respectively. In analogy to the assumptions of the previous section we consider a scattering process at rapidity  $Y$  with the source terms

$$q_0(y) = g_1\delta(y), \quad p_0(y) = g_2\delta(y - Y). \quad (25)$$

The action is invariant under the duality transformation

$$p \leftrightarrow q \quad \text{and} \quad y \rightarrow Y - y \quad (26)$$

for symmetric boundary conditions  $g_1 = g_2$  (obviously, the bulk action is invariant for any external couplings).

The classical trajectories  $\{q, p\}$  obey the equations of motion,

$$\partial_y q = \mu q - \lambda q^2 - 2\lambda q p, \quad (27)$$

$$-\partial_y p = \mu p - \lambda p^2 - 2\lambda q p \quad (28)$$

with the two-side initial conditions

$$q(0) = g_1, \quad p(Y) = g_2. \quad (29)$$

For  $g_1 < \mu/\lambda$  and  $g_2 < \mu/\lambda$  the classical trajectories are confined inside a triangle in the phase space spanned by points with  $(p, q)$  coordinates:  $(0, 0)$ ,  $(0, \mu/\lambda)$  and  $(\mu/\lambda, 0)$ . The problem possesses multiple solutions provided that rapidity  $Y$  is large enough. Thus, for  $Y$  smaller than a critical value  $Y_c$  (depending on  $g_1$ ,  $g_2$ ,  $\lambda$  and  $\mu$ ) there exists a unique solution,  $\{\bar{q}_1(y; g_1, g_2), \bar{p}_1(y; g_1, g_2)\}$ . In the case of  $g_1 = g_2 = g$  the solution preserves the symmetry between the target and the projectile,

$$\bar{q}_1(y; g, g) = \bar{p}_1(Y - y; g, g). \quad (30)$$

As in the case of PFT, above the critical rapidity  $Y_c$ , two more solutions  $\{\bar{q}_2(y; g, g), \bar{p}_2(y; g, g)\}$  and  $\{\bar{q}'_2(y; g, g), \bar{p}'_2(y; g, g)\}$  become possible which do not inherit the symmetry between the target and the projectile embedded in the action and the boundary conditions,

$$\bar{q}_2(y; g, g) \neq \bar{p}_2(Y - y; g, g) \quad \text{and} \quad \bar{q}'_2(y; g, g) \neq \bar{p}'_2(Y - y; g, g). \quad (31)$$

The three solutions are exemplified in Fig. 6(a) plotted in the phase space  $\{p, q\}$ . The parameters of the model were chosen to be  $\mu/\lambda=5$ ,  $g_1=g_2=0.7$ , and  $\mu Y = 8$ . For this rapidity, one finds the symmetric trajectory 1 and two asymmetric trajectories: 2 and 2'. At yet larger values of rapidity  $Y$  more solutions are possible, corresponding to cycles in the phase space and giving larger values of the action, so we neglect those cycles in the present analysis.

As in the case of PFT the emergence of the asymmetric solutions may be interpreted in terms of the spontaneous breaking of a discrete symmetry of the action. The symmetry between the target and the projectile is built in the action (23) and in the boundary conditions but some solutions of the equations of motion are not symmetric. This is possible, as the boundary conditions are defined at two points of rapidity and the classical solutions need not be unique. The symmetry, however, still holds for the full set of solutions,

$$\vec{q}'_2(y; g, g) = \vec{p}_2(Y - y; g, g) \quad \text{and} \quad \vec{p}'_2(y; g, g) = \vec{q}'_2(Y - y; g, g). \quad (32)$$

This means that under the duality transformation (26) each solution is transformed into itself (solution 1) or into another solution (solutions 2 and 2'), and the full set of solutions  $\{\vec{p}, \vec{q}\}$  is invariant under the duality transformation of  $p \leftrightarrow q$  and  $y \rightarrow Y - y$ .

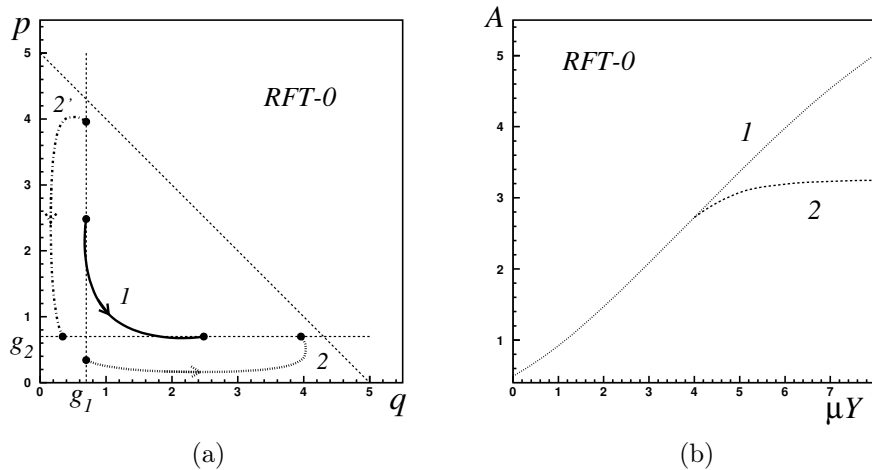


Fig. 6. Classical solutions of the RFT-0: (a) the  $\{q, p\}$  trajectories for  $Y > Y_c$ ; (b) value of the action  $\mathcal{A}_{\text{RFT-0}}[\vec{q}(y; g, g), \vec{p}(y; g, g); Y]$  for the symmetric solution (dotted line) and the asymmetric solution (dashed line) as a function of scaled rapidity  $\mu Y$ .

The observed phenomenon of spontaneous symmetry breaking occurs at the classical level. At the quantum level, however, the target-projectile symmetry should hold, as quantum transitions are possible between the states of the system corresponding to the classical trajectories. One sees it, for instance, from the form of the  $S$ -matrix in the semi-classical approximation using the three solutions  $\{1, 2, 2'\}$ . This corresponds to an evaluation of the

$S$ -matrix by applying the saddle-point method to the path integral:

$$S(Y; g_1, g_2) = \int [Dq Dp] \exp \{-\mathcal{A}_{\text{RFT-0}}[q(y), p(y); Y]\}. \quad (33)$$

Note, that the system evolves in rapidity which is formally equivalent to an evolution in the Euclidean time, thus the  $S$ -matrix is dominated by classical trajectories with the minimal value of the action. The value of the action corresponding to trajectories 1 and 2 is plotted in Fig. 6(b) as a function of the total rescaled rapidity  $\mu Y$ . Note, that trajectory 2 is only possible for  $Y > Y_c$ , and the critical rapidity  $\mu Y_c \simeq 4$  for our choice of parameters. Clearly, the value of the action is smaller for the asymmetric trajectories, therefore the asymmetric trajectories are expected to dominate the Euclidean path integral defining the scattering amplitude at large rapidities. The calculation of the quantum weights for  $Y > Y_c$  was performed in [20] leading to,

$$\begin{aligned} S(Y; g_1, g_2) \simeq & -\exp \{-\mathcal{A}_{\text{RFT-0}}[\bar{q}_1, \bar{p}_1; Y]\} \\ & + \exp \{-\mathcal{A}_{\text{RFT-0}}[\bar{q}_2, \bar{p}_2; Y]\} + \exp \{-\mathcal{A}_{\text{RFT-0}}[\bar{q}'_2, \bar{p}'_2; Y]\}, \end{aligned} \quad (34)$$

where the minus sign of the first term comes from the complex phase factors picked up by the trajectory 1 at the turning points. One sees that the symmetry between the target and the projectile is restored for the  $S$ -matrix already at the semi-classical level, by summation over the complete set of (asymmetric and symmetric) classical trajectories.

Finally, we have checked that the phenomenon of “fan dominance” at large rapidities that was found in the case of PFT occurs also in RFT-0. Thus, both the “fan dominance” and the breaking of the target-projectile symmetry seem to be generic properties of the eikonal interacting pomeron theories in the semi-classical approximation.

## 5. Concluding remarks

In this contribution a construction of interacting pomeron field theory was described that respects the symmetry between the target and the projectile. The theory treated in the semi-classical approximation leads to equations of motion for the pomeron field — the Braun equations. Above certain critical value of the total rapidity available in the scattering the target-projectile symmetry is broken for individual solutions, even though the boundary conditions are symmetric. This exhausts the definition of the spontaneous symmetry breaking at the classical level. At the quantum level, however, the target-projectile symmetry remains valid. It happens because

the  $S$ -matrix is determined by a complete weighted sum over all trajectories, and the action which determines the weights is symmetric. This is visible already in the semi-classical approximation (see *e.g.* (34)), where the contributions of asymmetric classical trajectories combine to yield a symmetric answer.

The symmetry of the  $S$ -matrix ensures that the inclusive observables are also symmetric. One should ask if there exist any observables that could serve as experimental signatures of the asymmetry between the target and the projectile in heavy ion collisions. Such measurements would have to break the quantum coherence and superselect one of the asymmetric classical solution in the classical measurement process. As a first guess we would propose investigation of the average transverse momentum  $\bar{p}_T = \sqrt{\langle p_T^2 \rangle}$  of the particles produced in central collisions of heavy ions as a function of rapidity  $y$  in the c.m.s. frame *on the event-by-event basis*. With the symmetry between the target and the projectile being preserved the observable  $\bar{p}_T(y)$  measured for individual events should be the same after changing the definition of rapidity  $y \rightarrow -y$ . If the symmetry is broken in the event, however,  $\bar{p}_T(y)$  should exhibit a clear trend. Certainly, in order to give an evidence of the symmetry breaking, such asymmetric events should occur much more frequently than fluctuations in a symmetric system.

A word of caution is necessary here. The analysis of PFT that we have performed is based on the semi-classical approximation and the assumption of eikonal pomeron couplings. Accuracy of both approximations is poorly controlled. Although there is some evidence that the semi-classical approximation may work reasonably well in RFT-0, this may be false in PFT. The issue of multiple pomeron couplings to a complex source is also rather obscure — strict results exist only for an elementary colour dipole. Thus, it requires more investigations to establish the validity of Braun equations in phenomenological applications, for instance in describing the dynamics of nucleus-nucleus collisions.

Finally, it would be rather important to systematically compare and relate PFT with the Colour Glass Condensate approach. In particular, a postulated equivalence of the two approaches should be proved (or disproved). In fact, in this moment the CGC approach seems to be more advanced in the treatment of quantum effects (or pomeron loops) and it should be fruitful to translate the developments of CGC into the language of PFT. On the other hand, the existing results in CGC correspond mostly to the case of an asymmetric scattering: a small and simple probe scattering off a large and complex target and, to our knowledge, the symmetric scattering problem of two large objects was not studied in depth yet, down to the level of explicit solutions. Therefore, a direct comparison of the CGC results and

the results of the analysis described in this contribution is not easy, as those results refer to very different processes. Thus, we would like to view the described approach to the high energy hadron scattering as complementary to the CGC approach.

Let me thank Sergey Bondarenko for a fruitful collaboration on the subject discussed in this lecture. I am grateful to the Organisers for the invitation and the opportunity to participate in the School. The support of the grant of the Polish State Committee for Scientific Research (KBN) No. 1 P03B 028 28 is gratefully acknowledged.

#### REFERENCES

- [1] J. Bartels, C. Ewerz, *J. High Energy Phys.* **9909**, 026 (1999); C. Ewerz, *Phys. Lett.* **B512**, 239 (2001); C. Ewerz, V. Schatz, *Nucl. Phys.* **A736**, 371 (2004); T. Bittig, C. Ewerz, *Nucl. Phys.* **A755**, 616 (2005).
- [2] M.A. Braun, *Phys. Lett.* **B483**, 115 (2000); *Eur. Phys. J.* **C33**, 113 (2004); *Phys. Lett.* **B632**, 297 (2006).
- [3] S. Bondarenko, L. Motyka, [hep-ph/0605185](https://arxiv.org/abs/hep-ph/0605185).
- [4] L.N. Lipatov, *Sov. J. Nucl. Phys.* **23**, 338 (1976) [*Yad. Fiz.* **23**, 642 (1976)]; E.A. Kuraev, L.N. Lipatov, V.S. Fadin, *Sov. Phys. JETP* **45**, 199 (1977) [*Zh. Eksp. Teor. Fiz.* **72**, 377 (1977)]; I.I. Balitsky, L.N. Lipatov, *Sov. J. Nucl. Phys.* **28**, 822 (1978) [*Yad. Fiz.* **28**, 1597 (1978)]; L.N. Lipatov, *Phys. Rep.* **286**, 131 (1997).
- [5] J. Bartels, *Z. Phys.* **C60**, 471 (1993); J. Bartels, M. Wüsthoff, *Z. Phys.* **C66**, 157 (1995).
- [6] A. Kovner, M. Lublinsky, *Phys. Rev. Lett.* **94**, 181603 (2005); J.P. Blaizot, E. Iancu, K. Itakura, D.N. Triantafyllopoulos, *Phys. Lett.* **B615**, 221 (2005); Y. Hatta, E. Iancu, L. McLerran, A. Staśto, D. N. Triantafyllopoulos, *Nucl. Phys.* **A764**, 423 (2006); C. Marquet, A.H. Mueller, A.I. Shoshi, S.M.H. Wong, *Nucl. Phys.* **A762**, 252 (2005).
- [7] I. Balitsky, *Nucl. Phys.* **B463**, (1996) 99.
- [8] Y.V. Kovchegov, *Phys. Rev.* **D60**, 034008 (1999); *Phys. Rev.* **D61**, 074018 (2000).
- [9] A.H. Mueller, *Nucl. Phys.* **B415**, 373 (1994).
- [10] J. Jalilian-Marian, A. Kovner, H. Weigert, *Phys. Rev.* **D59**, 014015 (1999); J. Jalilian-Marian, A. Kovner, A. Leonidov, H. Weigert, *Phys. Rev.* **D59**, 014014 (1999); E. Iancu, A. Leonidov, L.D. McLerran, *Nucl. Phys.* **A692**, 583 (2001); E. Iancu, A. Leonidov, L.D. McLerran, *Phys. Lett.* **B510**, 133 (2001); E. Iancu, L.D. McLerran, *Phys. Lett.* **B510**, 145 (2001); E. Ferreiro, E. Iancu, A. Leonidov, L. McLerran, *Nucl. Phys.* **A703**, 489 (2002).

- [11] A.H. Mueller, A.I. Shoshi, *Nucl. Phys.* **B692**, 175 (2004); E. Iancu, A.H. Mueller, S. Munier, *Phys. Lett.* **B606**, 342 (2005); E. Iancu, D.N. Triantafyllopoulos, *Nucl. Phys.* **A756**, 419 (2005); A.H. Mueller, A.I. Shoshi, S.M.H. Wong, *Nucl. Phys.* **B715**, 440 (2005); S. Munier, *Nucl. Phys.* **A755**, 622 (2005); E. Levin, M. Lublinsky, *Nucl. Phys.* **A763**, 172 (2005); E. Iancu, D.N. Triantafyllopoulos, *Phys. Lett.* **B610**, 253 (2005); R. Enberg, K. Golec-Biernat, S. Munier, *Phys. Rev.* **D72**, 074021 (2005); E. Iancu, C. Marquet, G. Soyez, [hep-ph/0605174](#).
- [12] R. Peschanski, *Acta Phys. Pol. B* **37**, 3511 (2006), these proceedings.
- [13] S. Munier, *Acta Phys. Pol. B* **37**, 3451 (2006), these proceedings, [[hep-ph/0609161](#)].
- [14] G. Soyez, *Acta Phys. Pol. B* **37**, 3477 (2006), these proceedings.
- [15] M.A. Braun, G.P. Vacca, *Eur. Phys. J.* **C6**, 147 (1999); J. Bartels, L.N. Lipatov, G.P. Vacca, *Nucl. Phys.* **B706**, 391 (2006).
- [16] C. Ewerz, *J. High Energy Phys.* **0104** (2001) 031.
- [17] K. Kutak, J. Kwieciński, *Eur. Phys. J.* **C29**, 521 (2003); K. Kutak, A.M. Staśto, *Eur. Phys. J.* **C41**, 343 (2005).
- [18] S. Munier, R. Peschanski, *Phys. Rev. Lett.* **91**, 232001 (2003); S. Munier, R. Peschanski, *Phys. Rev.* **D69**, 034008 (2004); S. Munier, R. Peschanski, *Phys. Rev.* **D70**, 077503 (2004).
- [19] D. Amati, L. Caneschi, R. Jengo, *Nucl. Phys.* **B101**, 397 (1975); V. Alessandrini, D. Amati, R. Jengo, *Nucl. Phys.* **B108**, 425 (1976); R. Jengo, *Nucl. Phys.* **B108**, 447 (1976); D. Amati, M. Le Bellac, G. Marchesini, M. Ciafaloni, *Nucl. Phys.* **B112**, 107 (1976); M. Ciafaloni, M. Le Bellac, G.C. Rossi, *Nucl. Phys.* **B130**, 388 (1977).
- [20] M. Ciafaloni, *Nucl. Phys.* **B146**, 427 (1978).
- [21] P. Rembiesa, A.M. Staśto, *Nucl. Phys.* **B725**, 251 (2005); A.I. Shoshi, B.W. Xiao, *Phys. Rev.* **D73**, 094014 (2006); M. Kozlov, E. Levin, [hep-ph/0604039](#); A.I. Shoshi, B.W. Xiao, [hep-ph/0605282](#); J.P. Blaizot, E. Iancu, D.N. Triantafyllopoulos, [hep-ph/0606253](#); S. Bondarenko, L. Motyka, A.H. Mueller, A.I. Shoshi, B.W. Xiao, [hep-ph/0609213](#); M. Kozlov, E. Levin, V. Khachtryan, J. Miller, [hep-ph/0610084](#).